UCLA
COMPUTATIONAL AND APPLIED MATHEMATICS

# Nonlinear Feedback Control of the Wake Past a Plate with a Suction Point on the Downstream Wall: From a Low-Order Model to a Higher-Order Model

L. Cortelezzi
Y.-C. Chen
H.-L. Chang

October 1995

CAM Report 95-44

Department of Mathematics
University of California, Los Angeles
Los Angeles, CA. 90024-1555

# Nonlinear feedback control of the wake past a plate with a suction point on the downstream wall: From a low-order model to a higher-order model. *

by L. CORTELEZZI,[1,2] † Y-C CHEN[2] and H-L CHANG[2]

[1] Department of Mathematics
University of California, Los Angeles, California 90095-1555
[2] Department of Mechanical, Aerospace, and Nuclear Engineering
University of California, Los Angeles, California 90095-1597

October 17, 1995

**Abstract**

Active circulation control of the two-dimensional unsteady separated flow past a plate with a suction point on the downstream wall is considered. A low-order point vortex model and a high-order vortex blob model are used to simulate the roll-up of the separated shear layer. A nonlinear controller able to confine the wake to a single vortex pair of constant circulation is given in closed form for the point vortex model. The control strategy is applied to the vortex blob model by defining a center of circulation. The topological equivalence of the phase spaces of the two models is verified. Finally, the two models are used to simulate the same flows using the same controller and the results are discussed.

*This research was supported by the Air Force Office for Scientific Research Grant # F49620-92-J-0279.

†Send correspondence to: Luca Cortelezzi, Department of Mathematics, University of California, Los Angeles, California 90095-1555, U.S.A. E-mail: crtlz@math.ucla.edu

# 1 Introduction

The interdisciplinary field of fluid flow control is attracting wide interest in the engineering community; see Gunzburger (1995), Bushnell (1992), and Gad-el-Hak & Bushnell (1991) for discussions and references. In particular, a deep understanding of the control strategies necessary to control flows past bluff bodies would find application in drag reduction, lift enhancement, noise and vibration control, mixing improvement, etc.

In recent years several experiments have been successful in modifying certain characteristics of the wake behind bluff and slender bodies, such as reduction or magnification of the wake thickness (Tokumaru & Dimotakis 1991), wake stabilization (Roussopoulos 1993), vortex cancelation (Koochesfahani & Dimotakis 1988), pattern reproduction (Ongoren & Rockwell 1988*a*, *b*, Gopalkrishnan *et al.* 1994), and lift enhancement (Rossow 1977, Slomski & Coleman 1993). In all these investigations the free-stream velocity was maintained constant, and quasi-steady results were achieved usually by moving the body or the actuator with a frequency scaled by the shedding frequency. In a more general situation, in which the free-stream velocity is time dependent, this approach is generally not sufficient to control the flow and a nonlinear control strategy is necessary.

The problem of actively controlling an unsteady fluid flow is in general nonlinear. A general framework to obtain a desired controller is not yet available. However, Cortelezzi *et al.* (1994) recently proposed, as a possible framework, to derive the controller using a hierarchy of mathematical models of increasing complexity. As a first step, one should start with a reduced model able to capture the dynamic features of the flow that one wants to control. See Cao and Aubry 1993, Rajaee *et al.* 1994, Cortelezzi *et al.* 1994. Typically, the reduced model is a low-dimensional nonlinear system governed by a set of ordinary differential equations, for example, a point vortex model with few vortices. There are several advantages working with a reduced model: First, it is easier to derive the desired control strategy. Second, the dynamical system analysis can be easily used to characterize the dynamics of the system. Finally, the control strategy derived for the reduced model might produce fast numerical algorithms, which are essential for controlling a real flow. In the following steps, one should apply the control strategy derived for the reduced model to higher or infinite dimensional models in order to capture the evolution of the flow more accurately. Such models could be, for example, a vortex blob model with hundreds or thousands of blobs, or the infinite dimensional model of the Navier-Stokes equations. The final and the more challenging step is to apply the derived control strategy to an experiment.

As proposed by Cortelezzi (1995) the process of transferring the control strategy from a low-dimensional model to a higher or infinite dimensional model and eventually to a real flow should be guided and supported by a dynamical system and time series analysis. In general, the control strategy should be transferable from a low-order model to the next high-order model provided that the phase space of the two models are topologically equivalent. In the unfortunate case when the two models are not dynamically equivalent, the differences in the structure of their respective phase spaces and the knowledge of the controller for the lower-order model should provide sufficient

information to design a controller that governs the dynamics of the higher-order model.

The present study demonstrates that it is possible to apply the control strategy derived for a low-dimensional model to a high-dimensional model. The test case is the active control of the wake past a plate perpendicular to an unsteady flow. In Section 2 we introduce two inviscid vortex models: The first, a low-dimensional point vortex model, simulates the unsteady separation from the tip of a plate by means of a pair of point vortices of time-dependent circulation (Brown and Michael 1954, Rott 1956, Cortelezzi and Leonard 1993). The circulation is predicted by an unsteady Kutta condition. The second, a high-dimensional vortex blob model, simulates the unsteady separation with a collection of vortices with a finite core introduced in the flow at appropriate time intervals near the tips of the plate (Sarpkaya 1975, Kiya and Arie 1977, Chein and Chung 1988, Krasny 1991).

In Section 3, we consider as a control actuator a suction point placed on the downstream wall of the plate. The control objective is to confine the wake to a single vortex pair of constant circulation. We recall the closed form solution of the controller for the point vortex model obtained by Cortelezzi (1995). The controller predicts, for any free-stream velocity, the suction necessary to inhibit the production of circulation when a vortex pair is present in the flow.

In Section 4, we define the center of circulation of an ensemble of vortices in the presence of a finite size body. In this paper the center of circulation is the liaison between the two models. It permits an ensemble of vortex to be treated blobs as a single point vortex preserving certain properties of the ensemble. Consequently, it permits extension of the results obtained for the point vortex model to the vortex blob model, and comparison of the results obtained from the vortex blob model to the results obtained from the point vortex model.

In Section 5, we verify the topological equivalence of the phase spaces of the two models. We accomplish this task by running a series of numerical experiments with the vortex blob model. The numerical experiments are designed using the information provided by the phase space of the point vortex model. The dynamical equivalence of the two models substantiate the hypothesis that the controller derived for the point vortex model is also able to control the dynamics of the vortex blob model.

Finally the results of two pairs of simulations are presented in section 6. Within each pair we compare the performance of the controller when it is applied to the point vortex model and to the vortex blob model. The first pair of simulations tests the ability of the controller to drive the system to a stable fixed point when the free-stream is constant. The second pair of simulations tests the ability of the controller to drive the system to a limit cycle when the free-stream velocity oscillates periodically.

## 2 Mathematical formulation

In this section we introduce two inviscid models to simulate high Reynolds number two-dimensional unsteady separated flows past a finite plate with a suction point on the downstream wall.

Following Cortelezzi's work (1995), we choose a frame of reference fixed to the plate so that the plate can be identified with the segment $[-2ia, 2ia]$ and the suction point of strength $s$ coincides

with the point $(0^+, 0)$. Then, the flow of an incompressible irrotational fluid around the plate can be analyzed using conformal mappings. Using the Joukowski transformation

$$z = \zeta - \frac{a^2}{\zeta}, \tag{1}$$

we map the finite plate of length $L = 4a$ in the z-plane onto the circle of radius $a$ in the $\zeta$-plane (see Figure 1), preserving the characteristic of the flow at infinity.

To make the problem dimensionless we have to define a characteristic length and time scale. For this purpose we write the free-stream velocity as follows:

$$U(t) = U_\infty + u(t), \tag{2}$$

where $U_\infty$ is the unperturbed free-stream velocity and $u(t)$ is the time dependent component. Choosing the circle radius as the characteristic length and $a/U_\infty$ as the characteristic time of the problem, we define the following dimensionless quantities:

$$\begin{aligned} z^* &= \frac{z}{a}, & \zeta^* &= \frac{\zeta}{a}, & a^* &= 1, & t^* &= \frac{U_\infty t}{a}, \\ U^* &= \frac{U}{U_\infty} = 1 + \epsilon_U, & \Gamma^* &= \frac{\Gamma}{U_\infty a}, & s^* &= \frac{s}{U_\infty a}, \end{aligned} \tag{3}$$

where $\Gamma$ is the circulation. Note that $\epsilon_U = u/U_\infty$ contains the unsteadiness of the free-stream velocity and is not necessarily small with respect to unity. From this point on, we continue the mathematical formulation of the problem using dimensionless variables, where the stars are omitted for convenience.

Since the velocity field has to satisfy Laplace's equation and the boundary condition in the mapped plane can be treated using the Circle Theorem, we can build the complex potential $F$ by superimposing basic flows. Thus, the complex velocity field $w = dF/d\zeta$ has the form

$$\begin{aligned} w(\zeta, t) = {} & U\left(1 - \frac{1}{\zeta^2}\right) - s\frac{\zeta + 1}{\zeta(\zeta - 1)} \\ & + \frac{i\Gamma_1^t(t)}{2\pi}\left(\frac{1}{\zeta - \zeta_1^t} + \frac{\bar{\zeta}_1^t}{1 - \zeta\bar{\zeta}_1^t} + \frac{1}{\zeta}\right) + \sum_{n=2}^{N^t} \frac{i\Gamma_n^t}{2\pi}\left(\frac{1}{\zeta - \zeta_n^t} + \frac{\bar{\zeta}_n^t}{1 - \zeta\bar{\zeta}_n^t} + \frac{1}{\zeta}\right) \\ & + \frac{i\Gamma_1^b(t)}{2\pi}\left(\frac{1}{\zeta - \zeta_1^b} + \frac{\bar{\zeta}_1^b}{1 - \zeta\bar{\zeta}_1^b} + \frac{1}{\zeta}\right) + \sum_{n=2}^{N^b} \frac{i\Gamma_n^b}{2\pi}\left(\frac{1}{\zeta - \zeta_n^b} + \frac{\bar{\zeta}_n^b}{1 - \zeta\bar{\zeta}_n^b} + \frac{1}{\zeta}\right). \end{aligned} \tag{4}$$

In the above expression we have the free-stream velocity, $U$, the suction strength, $s$, $N^t$ vortices shed by the top tip at $\zeta = \zeta_n^t$ with their images within the circle, and $N^b$ vortices shed by the bottom tip at $\zeta = \zeta_n^b$ and their images within the circle. Note that for convenience we take the circulation to be positive when in clockwise sense, contrary to the usual convention. Note also that the singularity on the back face of the plate behaves as a sink when $s > 0$ and as a source otherwise. We impose the Kutta condition to regularize the potential flow at the tips of the plate. In the $\zeta$-plane the flow is non-singular since the singularity has been absorbed by the mapping. To remove the singularity in the $z$-plane, the complex velocity (4) in the mapped plane has to be zero at the top and the bottom

of the circle. In other words, the circulation $\Gamma_1^t$ and $\Gamma_1^b$ of the new vortices is obtained by solving the following equations:

$$\begin{cases} w(i,t) = 0, \\ w(-i,t) = 0. \end{cases} \tag{5}$$

## 2.1 Point vortex model

In this subsection we introduce a low-dimensional model, also referred to as a reduced model, of two-dimensional unsteady separated flows past a finite plate. We assume that the regions of vorticity that separate from the boundary layer and are convected away are thin enough to justify a description by means of a vortex sheet. The consequent stretching and rolling up of the vortex sheet, due to the unsteadiness of the flow, suggests a more coarse description via point vortices (see Brown and Michael 1954, Rott 1956, Cortelezzi and Leonard 1993). The vortex sheet is not completely lost. It is assumed to be of negligible circulation and connects the tip of the plate to a point vortex of time-dependent circulation which is able to satisfy an unsteady Kutta condition. The mathematical representation of the feeding vortex sheet is simply the branch cut due to the logarithmic singularity representing the vortex. All the other vortices in the wake are represented by point vortices of fixed circulation.

There is experimental evidence (Lisosky 1993) that the near wake is nearly two dimensional and symmetric about the x-axis if the plate moves with a nonzero acceleration. Under these circumstances the problem can be simplified by imposing symmetry with respect to the real axis, i.e., by requiring that the vortices have equal and opposite circulation, $\Gamma_n^t = \Gamma_n$ and $\Gamma_n^b = -\Gamma_n$, and are located in complex conjugate positions, $\zeta_n^t = \zeta_n$ and $\zeta_n^b = \bar{\zeta_n}$, respectively.

To describe the motion of the vortex pairs in the physical plane we use the following set of ordinary differential equations:

$$\begin{cases} \dfrac{d\bar{z}_1}{dt} + (\bar{z}_1 + 2i)\dfrac{1}{\Gamma_1}\dfrac{d\Gamma_1}{dt} = \lim\limits_{z \to z_1} \left\{ \dfrac{d}{dz}\left[ F - \dfrac{i\Gamma_1}{2\pi}\log(z - z_1) \right] \right\} \\ \dfrac{d\bar{z}_r}{dt} = \lim\limits_{z \to z_r} \left\{ \dfrac{d}{dz}\left[ F - \dfrac{i\Gamma_r}{2\pi}\log(z - z_r) \right] \right\}, \qquad r = 2, ..., N, \end{cases} \tag{6}$$

with the initial conditions:

$$\begin{cases} z_1(t_s) = 2i \\ z_r(t_s) = z_{r_s} \qquad r = 2, ..., N. \end{cases} \tag{7}$$

The top equation of motion predicts the position of the vortex pair of time-dependent circulation and the term containing $d\Gamma_1/dt$ is known as Brown and Michael's correction (Brown and Michael 1954). The limit on the right hand side, which represents the complex velocity at the vortex location without the self-induced contribution, produces the so called "Routh's correction" when it is evaluated in the mapped plane (e.g. Clements 1973). The bottom $N-1$ equations of motion predict the position of the vortex pairs of constant circulation. $t_s$ indicates the time when the rate of circulation production is zero. Up to time $t_s^-$ the circulation of the vortex pair 1 changes to satisfy the Kutta condition.

At time $t = t_s$ this vortex pair has is circulation frozen and all the vortices are renumbered. At $t_s^+$ a new vortex pair 1 on time-dependent circulation is introduced in the flow.

The reader is referred to Cortelezzi's work for a detailed implementation of this model (see Cortelezzi 1995).

## 2.2 Vortex blob model

In this subsection we introduce a high-dimensional model, a vortex blob model (Chorin 1973), of two-dimensional unsteady separated flows past a finite plate. We assume, as in the previous model, that the regions of vorticity that separate from the boundary layer and are convected away are thin enough to justify a description by means of a vortex sheet. The vortex sheet is represented by a collection of vortices with finite cores, also known as vortex blobs, introduced into the flow at appropriate time intervals near the tips of the plate. The evolution of the vortex sheet is then approximated by the motion of the vortex blobs.

The concept of vortex blobs was introduced to simulate slightly viscous effects in an inviscid environment (see Chorin 1973). Practically, the vortex blob concept permits to reduce the unrealistic high velocity induced on each vortex when two vortices get too close to each other. The blob size represent a cutoff. Within the blob, the velocity field approximates the velocity field in the core of a viscous vortex. Outside the blob, the velocity field coincides with the velocity field of a point vortex. Several blob shapes have been suggested by different authors, see Sarpkaya 1989 for references. In our simulation we use an algebraic blob profile suggested by Hald (1979).

The motion of the blobs is predicted by the following equations:

$$\begin{cases} \dfrac{d\bar{z}_p^t}{dt} = \lim\limits_{z \to z_p^t} \left\{ \dfrac{d}{dz} \left[ F - \dfrac{i\Gamma_p^t}{2\pi} \log(z - z_p^t) \right] \right\}, & p = 1, ..., N^t, \\ \dfrac{d\bar{z}_q^b}{dt} = \lim\limits_{z \to z_q^b} \left\{ \dfrac{d}{dz} \left[ F - \dfrac{i\Gamma_q^b}{2\pi} \log(z - z_q^b) \right] \right\}, & q = 1, ..., N^b. \end{cases} \tag{8}$$

We integrate these equations in time using a $4^{th}$ order Runge-Kutta scheme. A pair of new vortices is introduced in the flow domain at each time step. Note that the circulation of the new vortices, $\Gamma_1^t$ and $\Gamma_1^b$, does not depend on time since it remains fixed once the vortices are introduced in the fluid domain.

Vortex blob models are used quite commonly in the literature, see Sarpkaya 1989 for references and discussion. Hence, we will keep short the discussion about the implementation of the vortex blob model. Only the separation at the tips of the plate and the suction point deserve attention.

The separation mechanism at the tips of the plate has to be implemented with care because it affects the final quality of the simulation. Different techniques have been proposed in the literature, see Sarpkaya 1989 for references and discussion. We approach the problem in a semi-classical fashion: Up to time $t = 0.1$ we use a pair of point vortices of time-dependent circulation. In other words, we use the point vortex model to start up the vortex blob simulation. At initial times, in fact, the separation is especially difficult to simulate with the vortex blob model because there are only few vortex blobs in the flow and it is not clear where they should be placed. For $t > 0.1$ we use the first

sub-step of the Runge-Kutta routine to place the new vortex blob in the flow while we are convecting all the other. The circulation of the new vortex blob is determined by imposing the Kutta condition (5). The new vortex blob is placed in the flow at a distance from the tip of the plate predicted by a two points velocity measurement taken around the tip of the plate. Then, the new vortex blob is convected for the remaining three sub-steps of the Runge-Kutta routine like all the other vortex blobs. Consequently, the position of the new vortex blob after one time step is being improved and corrected during the three sub-steps. We choose as blob size $\sigma = 0.01$. This choice is a compromise between the need to reduce the high velocities generated by small vortex blobs and the need to avoid the overlapping of the vortex blobs with the plate.

The suction point is mathematically defined as a logarithmic singularity. Consequently, vortex blobs convected near the suction point experience high velocities. This phenomenon may generate numerical errors if it is not handled properly. Sometimes, in fact, a vortex blob in the neighborhood of the suction point is unrealistically convected very far away instead of disappearing into the plate. To avoid this problem we encircled the suction point with a circle of radius $\delta = 0.05L$. At each sub-step of the Runge-Kutta routine we check for vortex blobs within the circle. If a vortex blob is present and at the next sub-step is convected outside the circle then we force the blob to disappear into the plate.

# 3 Active wake control

In this section we introduce a nonlinear controller which is able to confine the wake behind the plate to a single vortex pair of constant circulation. The controller is derived for the point vortex model. In the following sections we will show that the controller can be successfully implemented also in a vortex blob model.

There are different approaches one can use to control the wake past a plate by suction. One may try to control the position of the vortices or some features of the velocity field. We choose to control the amount of circulation injected in the flow since we believe that this is the most efficient way to control the wake. As shown by Cortelezzi, suction and its rate of change contribute to the production of circulation in the same way as free-stream velocity and free-stream acceleration do (see Cortelezzi 1995). Hence, using suction as a mean to control the rate of circulation production is as powerful as using the free-stream velocity.

Our control objective is to inhibit the rate of circulation production after the starting vortex pair is shed in the flow. In other words, we want to predict the suction so that once the starting vortex pair is shed in the flow the Kutta condition remains satisfied without requiring a new vortex pair. The possibility to maintain the wake confined to a controlled recirculating bubble has an important implication to the general problem of drag reduction. Moreover, it can provide insight into vortex management techniques for the three-dimensional flow over a delta wing (see Rao 1987).

The controller closed form solution was obtained by Cortelezzi (1995). Let $t_s$ be the time when the starting vortex pair is shed in the flow, i.e., the time when the rate of circulation production is

zero. Then the suction which implements our control strategy is

$$s = -2U - \pi i \Gamma_{1_s} \frac{(\zeta_1 - \bar{\zeta}_1)(1 - \zeta_1 \bar{\zeta}_1)}{(1 + \zeta_1^2)(1 + \bar{\zeta}_1^2)}, \qquad \forall t \geq t_s, \tag{9}$$

where $\Gamma_{1_s}$ is the constant circulation associated with the vortex pair.

# 4 Center of circulation

Here we introduce the center of circulation of an ensemble of vortices in the presence of a finite size body. In this paper, the center of circulation is the liaison between point vortex model and vortex blob model. It allows us to treat an ensemble of vortex blobs as a single point vortex. Consequently, we are able to extend the results obtained for the point vortex model to the vortex blob model, and to compare the results obtained from the vortex blob model to the ones obtained from the point vortex model.

In literature, the concept of the center of circulation has been used mainly to amalgamate two or more vortices. As noticed by Sarpkaya, "the reasons for amalgamating vortices are common to many vortex method schemes: Often it is necessary to reduce the unphysically large velocities induced in each other, to limit their propensity to orbit about each other, to simulate more closely some naturally occurring merging, and to reduce computer time" (see Sarpkaya 1989). Sarpkaya also underlines the fact that it has been customary to combine $N$ vortices of circulation $\Gamma_i, i = 1, ..., N$ and position $\zeta_i, i = 1, ..., N$ into a single vortex of strength

$$\Gamma_m = \sum_{i=1}^{N} \Gamma_i, \tag{10}$$

placed at their center of circulation, given by

$$\zeta_{mi} = \frac{1}{\Gamma_m} \sum_{i=1}^{N} \Gamma_i \zeta_i. \tag{11}$$

In other words, the center of circulation can be envisioned as a point vortex of circulation $\Gamma_m$ positioned at $\zeta_{mi}$.

This definition of center of circulation conserves total circulation and linear momentum only when the fluid domain is unbounded or when the boundary of the problem can be mapped onto a straight line. The error introduced in the complex velocity field by the amalgamation scheme decays as $\sim \zeta^{-3}$ far from the merging location. Instead, when the amalgamation process takes place in the presence of a finite size body, the above scheme conserves only the total circulation while the linear momentum of the system is not conserved in general. Consequently, the error induced on the velocity field decays only as $\sim \zeta^{-2}$. A finite size body in principle can always be mapped onto a unit circle and using the circle theorem it is easy to show that the image of the center of circulation in general does not coincide with the center of circulation of the $N$ vortex images (see Cortelezzi 1993).

To conserve both total circulation and linear impulse and to produce an error $\sim \zeta^{-3}$ in the complex velocity field when a body of finite size is present into the flow, it is necessary to consider the contribution of vortices and their images. In this case, the center of circulation is obtained by solving the following equation:

$$\Gamma_m \left( \zeta_{mf} - \frac{1}{\bar{\zeta}_{mf}} \right) = \sum_{i=1}^{N} \Gamma_i \left( \zeta_i - \frac{1}{\bar{\zeta}_i} \right), \tag{12}$$

where $\Gamma_m$ is defined by (10). This equation guarantees that the linear momentum of the center of circulation and its image equal the linear momentum of the ensemble of vortices and their images. The center of circulation has the following expression:

$$\zeta_{mf} = \sqrt{\frac{I_m}{\bar{I}_m}} \left[ \frac{\sqrt{I_m \bar{I}_m + 4a^2\Gamma_m^2} + \sqrt{I_m \bar{I}_m}}{2\Gamma_m} \right]. \tag{13}$$

To use this definition effectively, the amalgamation process has to take place sufficiently far from the body. Unfortunately, because of the reasons stated in the beginning of this section, the merging process has to take place even when the vortices are not that far from the body. Consequently, a significant time-dependent perturbation is introduced in the velocity field near the body, and particularly near the separation points. In other words, the effect of the merging process is instantaneously fed back to the body, hence making the separation process rather noisy.

To avoid this problem one could propose a completely different definition of center of circulation which does not modify the rate of circulation production. Unfortunately, the mathematics involved discourages any attempt to impose such a condition. A reasonable compromise is to impose the condition that the velocity field at the separation point is not affected by the merging process. In general, only two constraints can be imposed, one of which must be the conservation of circulation. Consequently, it is necessary to choose whether it is more appropriate to impose the conservation of the linear impulse or to maintain the velocity at the separation points unchanged. However, in there exists an axis of symmetry (the real axis in our study) three constrain can be imposed. In this particular case, we can impose the conservation of the linear impulse and also maintain the velocity at the separation points unchanged, with the following equations:

$$\begin{cases} \Gamma_m \dfrac{(\zeta_{mk} - \bar{\zeta}_{mk})(a^2 - \zeta_{mk}\bar{\zeta}_{mk})}{\zeta_{mk}\bar{\zeta}_{mk}} = \displaystyle\sum_{i=1}^{N} \Gamma_i \frac{(\zeta_i - \bar{\zeta}_i)(a^2 - \zeta_i\bar{\zeta}_i)}{\zeta_i\bar{\zeta}_i}, \\ \Gamma_m \dfrac{(\zeta_{mk} - \bar{\zeta}_{mk})(a^2 - \zeta_{mk}\bar{\zeta}_{mk})}{(a^2 + \zeta_{mk}^2)(a^2 + \bar{\zeta}_{mk}^2)} = \displaystyle\sum_{i=1}^{N} \Gamma_i \frac{(\zeta_i - \bar{\zeta}_i)(a^2 - \zeta_i\bar{\zeta}_i)}{(a^2 + \zeta_i^2)(a^2 + \bar{\zeta}_i^2)}, \end{cases} \tag{14}$$

where $\Gamma_m$ is defined by (10). These two equations determine uniquely the center of circulation. For convenience we define the quantities:

$$\begin{aligned} K &= \sum_{i=1}^{N} \Gamma_i \frac{2\eta_i(1-\rho_1^2)}{1 + 2(\rho_i^2 - 2\eta_i^2) + \rho_i^4} & L &= \sum_{i=1}^{N} \Gamma_i \frac{\eta_i(1-\rho_i^2)}{\rho_i^2} \\ A &= LK(LK - 2\Gamma_m^2) & B &= (L^2 + 2\Gamma_m^2)K - \Gamma_m^2 L \end{aligned} \tag{15}$$

where $\eta_i$ and $\rho_i$ are the ordinate and radius of the vortex position $\zeta_i$, i.e. , $\zeta_i = \xi_i + i\eta_i = -i\rho_i e^{i\theta_i}$ (see Figure 1). The above equations have a solution only if $A \geq 0$ and it is given by

$$\zeta_{mk} = \begin{cases} \sqrt{\dfrac{\Gamma_m \eta_{mk}}{\Gamma_m \eta_{mk} + L} - \dfrac{1}{4\Gamma_m^2}\left[\sqrt{\dfrac{B+L\sqrt{A}}{2K}} + \sqrt{\dfrac{B-L\sqrt{A}}{2K}} + L\right]^2} \\ \qquad - \dfrac{i}{2\Gamma_m}\left[\sqrt{\dfrac{B+L\sqrt{A}}{2K}} + \sqrt{\dfrac{B-L\sqrt{A}}{2K}} + L\right] \qquad \Gamma_m < 0, \\ \sqrt{\dfrac{\Gamma_m \eta_{mk}}{\Gamma_m \eta_{mk} + L} - \dfrac{1}{4\Gamma_m^2}\left[\sqrt{\dfrac{B+L\sqrt{A}}{2K}} + \sqrt{\dfrac{B-L\sqrt{A}}{2K}} - L\right]^2} \\ \qquad + \dfrac{i}{2\Gamma_m}\left[\sqrt{\dfrac{B+L\sqrt{A}}{2K}} + \sqrt{\dfrac{B-L\sqrt{A}}{2K}} - L\right] \qquad \Gamma_m > 0. \end{cases} \tag{16}$$

In the following section we will use the latter definition of center of circulation to relate the vortex blob model to the point vortex model. For an amalgamation scheme based on the latter definition of center of circulation see Cortelezzi 1993.

# 5 Phase space of the vortex blob model

The application of a controller derived for a low-dimensional model to a model of higher or of infinite dimension is not trivial. Beside the old trial-and-error method a better and more scientific approach is to prove or to verify that the two models are dynamically equivalent; namely, that the phase spaces of the two models are topologically equivalent. If the two models are dynamically equivalent then the controller designed to govern the dynamics of the low-order model should, in principle, be able to govern the dynamics of the of the higher-order model. If, instead, the two models are not dynamically equivalent then the differences in the structure of their respective phase spaces and the knowledge of the controller for the lower-order model should provide the necessary information for designing a controller to govern the dynamics of the higher-order model.

The proof of the dynamic equivalence of the point-vortex and the vortex-blob models can be given by deriving the equation of motion for the center of circulation. Even though non trivial, the derivation of the equation of motion for the center of circulation is, in principle, possible. When the equation of motion for the center of circulation is available it can be analyzed as a dynamical system; i.e., we can compute its fixed points, limit cycles, etc. and study their structure and stability. The final step of this process is the construction of the phase space associated with the dynamics of the center of circulation and the comparison with the phase space associated with the dynamics of the point vortex. If the phase spaces of the two systems present the same types of fixed points, limit cycles, etc., then the two models are dynamically equivalent and the controller derived for the reduced model should, in principle, govern the dynamics of the higher-order system.

A less formal approach, the one taken in this study, is the numerical verification of the topological equivalence of the phase spaces. To verify the equivalence of the phase spaces one should run a series of numerical experiments to confirm that the controller is able to drive the system, for example, near a stable fixed point of the reduced model. The numerical experiments are suggested, of course, on the basis of the knowledge of the phase space of the reduced model. A methodic reconstruction of the phase space of the higher-order model would provide crucial information about performance and limitation of the controller and possible suggestions in case the controller has to be redesigned.

The phase space structure of the point vortex model has been studied in detail by Cortelezzi (1995). The point vortex model presents fixed points only when the suction is nonzero (fixed points are those where the vortex is stationary when the free-stream velocity is unity and suction is constant). The locus of the fixed point is shown by the solid curve in Figure 2. Each point on this curve represents the position of a vortex which is stationary and satisfies the Kutta condition, and whose circulation is shown by the solid curve in Figure 3(b). The suction associated with each fixed point is shown by the solid curve in Figure 3(a). The reader should be aware that the discussion is restricted to the upper half of the domain due to the symmetry of the problem. Linear stability analysis shows that the fluid domain downstream the plate presents three stability regions. When $x < x_1$ the fixed points are unstable foci, when $x_1 < x < x_2$ they are stable nodes, and when $x > x_2$ they are saddle points (see Figure 2). We restrict our discussion to the sub-domain where $x > x_1$, $\Gamma_{1_s} > 0$, and $s > 0$. It is important to observe that in this sub-domain there are fixed points only when $\Gamma_{1_s} \geq \Gamma_c$. The circulation plays the role of a bifurcation parameter and the vector field undergoes a saddle-node bifurcation at $x = x_2$ when $\Gamma_{1_s} = \Gamma_c$.

We conducted a series of numerical experiments with the vortex blob model to verify the existence of stable fixed points and their locus (fixed points now being those where the center of circulation is stationary when the free-stream velocity is unity and suction is constant). The complexity of the two system is entirely different: the point vortex model uses only 2 vortices where the vortex blobs model uses more than 1000 blobs. Note also that although no symmetry was imposed on the blob model, the resulting simulations were symmetric with respect to the real axis.

The numerical experiments were designed using the information provided by the phase space of the point vortex model. The free-stream velocity reaches a unit value after an initial transient necessary for the formation of the vortex (see Figure 4). The amplitude of the initial transient was modified to generate vortices of the desired circulation. Suction was set to the value predicted by Figure 3(a). The experiments were stopped when there was evidence that the system had reached a steady state. The outcome of the experiments is presented in Figures 2 and 3 using symbols. Figure 2 compares the stability regions of the two models. There is a good agreement in the location of the fixed points although the stability region of the vortex blob model appears to be slightly wider than that of the point vortex model. The symbol further downstream indicates the location of the fixed point when the circulation nearly equals $\Gamma_c$. Vortices with circulation lower than $\Gamma_c$ drift irreversibly downstream. Analyzing Figure 2, one can argue that the stability region of the vortex blob model extends also upstream with respect to the stability region of the point vortex model. We cannot confirm this hypothesis because we were not able to detect any fixed point of the left of $x_1$. High values of circulation require intense suction and in these cases vortex blobs are continuously sucked

into the plate reducing the total circulation. Figure 3(a) presents a comparison between the suction used by the two models to generate fixed points. Figure 3(b) presents a comparison between the circulation of the top point vortex and the circulation associated with the top center of circulation when the steady state is reached. Both figures show a good agreement between the two models. Figure 3(b) shows that the circulation associated with the center of circulation plays the role of a bifurcation parameter, and the bifurcation value is approximately $\Gamma_c$. This is a crucial evidence of the dynamic equivalence of the two models. It guarantees, in fact, that both models present the same number and type of fixed points. Finally, Figure 3 substantiate the hypothesis that the region of stability of the vortex blob model is slightly wider of the region of stability of the point vortex model.

The evidence provided by Figures 2 and 3 is sufficient to conclude that the phase space of the two models are indeed topologically equivalent when free-stream velocity and suction are constant. When the free-stream velocity is unsteady the dynamic equivalence of the two models should be verified using the Poincaré section. This step is not necessary in our case thanks to a theorem (see Guckenheimer and Holmes, Chp. 4) which guarantees that the Poincaré section of a periodically perturbed system is topologically equivalent to the phase space of the unperturbed system, provided that the fixed points are hyperbolic and the perturbations are sufficiently small. Since both models present the same hyperbolic fixed points and since these fixed points nearly coincide, it follows that the Poincaré sections of the two models nearly coincide. Consequently, it is reasonable to expect that the controller derived for the point vortex model should control the dynamics of the higher dimensional vortex blob model.

# 6 Results

In this section we present the results of two simulations. We ran each simulation twice. The first time we used the point vortex model and the second time the vortex blob model. In both cases we used exactly the same free-stream velocity and the same controller, the one derived for the point vortex model (see Section 3). In the first case we fed back to the controller the position and circulation of the point vortex while in the second case we fed back to the controller the position and circulation of the center of circulation.

In the first simulation, the free-stream velocity increases from rest, reaches a maximum value, and decreases to a unit value at $t = 1$ (see Figure 4). We carefully choose the initial evolution of the free-stream velocity so that, in both simulations, a vortex pair of nearly the same circulation $\Gamma_{1_s} > \Gamma_c$ is shed in the flow at nearly the same time. For simplicity, suction is used to control the wake only after the rate of circulation production decreased to zero (see Figures 6 and 7). Figure 5 shows the comparison between the trajectory of the point vortex and the trajectory of the center of circulation. The trajectories are nearly the same and both, point vortex and center of circulation, are driven to nearly the same fixed point. The comparison between the circulation of the top point vortex and circulation of the top center of circulation is also satisfactory (see Figure 7). The controller works, of course, perfectly with the point-vortex model, but it also maintains the circulation of the

vortex blob simulation near the desired constant value $\Gamma_{1_s}$. The slight difference in the circulation amplitudes is probably due to the different integration time step used in the two schemes. It is interesting to compare the control signals, i.e., the suction required by the two models, as a function of time (see Figure 6). The suction required by the vortex blob model follows quite closely the suction required by the point vortex model. The slight difference in amplitude is a consequence of the slight difference in the respective circulations (see Figure 3). The noise that affects the control signal is probably generated by the need to compensate for the rotation and the deformation of the ensemble of vortex blobs. Figure 8 presents a comparison between the stream function of the two simulations at different times during the capture of the vortex pair. The two simulations differ on the symmetry conditions: no symmetry was imposed on the vortex blob simulation while the point vortex simulation is strictly symmetric. Nevertheless, the two simulations are nearly identical and symmetric, consequently only the top half of the domain is shown. Figures 6(a)-(d) show the flow at time $t < t_s$, where two recirculating bubbles grow and merge together. As suction becomes non-zero the recirculating bubble is newly splitted in two bubbles, see Figures 6(e) and (f). Figures 6(e)-(l) show how the vortex and the center of circulation are driven to the respective fixed points. Finally, Figures 6(i)-(l) show the flow near the steady state.

In the second simulation the free-stream velocity increases from rest and reaches a maximum value, as in the first simulation, but then oscillates about unit mean value (see Figure 9). The amplitude of the oscillation is 0.7 which represents a substantial perturbation with respect to the previous case (see Figure 4). Three distinct intervals of time can be recognized. Initially, when $0 < t < t_s$, the flow behaves qualitatively as in the first simulation. In the second interval, $t_s < t < 2$, the controller drives the vortex in the neighborhood of the limit cycle trajectory. Finally, when $t > 2$, the transient behavior decays rapidally and the vortex moves on the limit cycle trajectory. Figure 10 shows the comparison between the trajectory of the point vortex and the trajectory of the center of circulation. The trajectories are nearly the same and both, point vortex and center of circulation, are driven almost to the same limit cycle trajectory. The comparison between the circulation of the top point vortex and the circulation of the top center of circulation is again satisfactory (see Figure 12). The difference in amplitude can be explained as in the previous case. The circulation of the center of circulation presents a periodic indentation. The indentations are due to the loss of few vortex blobs during the cyclic acceleration. However, the circulation quickly relaxes to the desired constant value $\Gamma_{1_s}$, thus providing some evidence of the robustness of the controller. Figure 11 shows the comparison between the two control signals. Overall, the suction required by the vortex blob model follows quite closely the suction required by the point vortex model. On one hand, there is an excellent agreement during the cyclic deceleration. On the other hand, the suction required by the vortex blob model becomes noisy during the cyclic acceleration probably because of the variation in rotation and shape of the ensemble of vortex blobs. Figure 13 presents a comparison between the stream function of the two simulations during one period of oscillation, $6 < t < 8$, as the vortices move clockwise on the limit cycle trajectory.

We would like to conclude by pointing out that the point vortex simulation involves only 2 vortices while the vortex blob simulation involves about 1000 blobs. The instantaneous stream functions are remarkably similar, only the size of the vortex core, in black, is clearly different (see Figures 11 and

13). In the vortex blob simulation the vortex core occupies large part of the recirculation region due to the distribution of blobs over the region, while in the point vortex simulation the stream function peaks at the location of the point vortex.

# 7 Conclusions

Two inviscid vortex models, a low-order point vortex model and a high-order vortex blob model, have been used to simulate two-dimensional unsteady separated flows past a flat plate with a suction point on the downstream wall. For the point vortex model we introduced a control strategy that confines the wake to a single vortex pair of constant circulation. We reported the analytical closed form solution of the nonlinear controller for any free-stream conditions. We defined a center of circulation in order to apply the control strategy obtained for the point vortex model to the vortex blob model. The transferability of the control strategy was justified by verifying the topological equivalence of the phase spaces of the two models. The two models share the same bifurcation parameter, the circulation. The vector field of both models undergoes to a saddle-node bifurcation at nearly the same value of the bifurcation parameter. We also inferred the topological equivalence of the Poincaré section of the the two models when the free-stream oscillates in time. The transferability of the control strategy was finally tested on two flow simulations using the same controller for both models. The first simulation documented the ability of the controller to drive the vortex pair to the stable nodes when the free-stream is asymptotically constant. The second simulation documented the ability of the controller to drive the vortex pair to the periodic orbits when the free-stream velocity oscillates periodically about a unit mean. In both cases the controller which was derived for the point vortex model was controlled satisfactorily the dynamics of the vortex blob model.

The present study showed that it is possible to transfer the control strategy derived for a low-order model to a higher-order model. The natural continuation of the present work would be to embed the controller derived for the point vortex model into an infinite-dimensional model, for example, the Navier-Stokes equations. The embedding process should again be supported and guided by a dynamical system and time series analysis to demonstrate the dynamical equivalence of the two models. Testing the controller in a different numerical environment instead of an experiment presents several advantages: All the flow quantities necessary to feedback to the controller can be easily measured. The action of the controller is automatically synchronized with the evolution of the flow. Finally, the controller can be easily tested on gradually more complex flows allowing the researcher to make the controller progressively robust with respect to different types of perturbations (e.g. viscosity, three-dimensionality, back-ground noise, etc.). Successful completion of this process would open the possibilities for the active control of large-scale coherent vortical structures in engineering applications.

# 8 Acknowledgments

The authors wish to thank Dr. J.S. Gibson for the many enlighting discussions. The authors also wish to thank Dr. C.R. Anderson and Dr. J.S. Gibson for the financial support. This research was supported by the Air Force Office for Scientific Research Grant # F49620-92-J-0279.

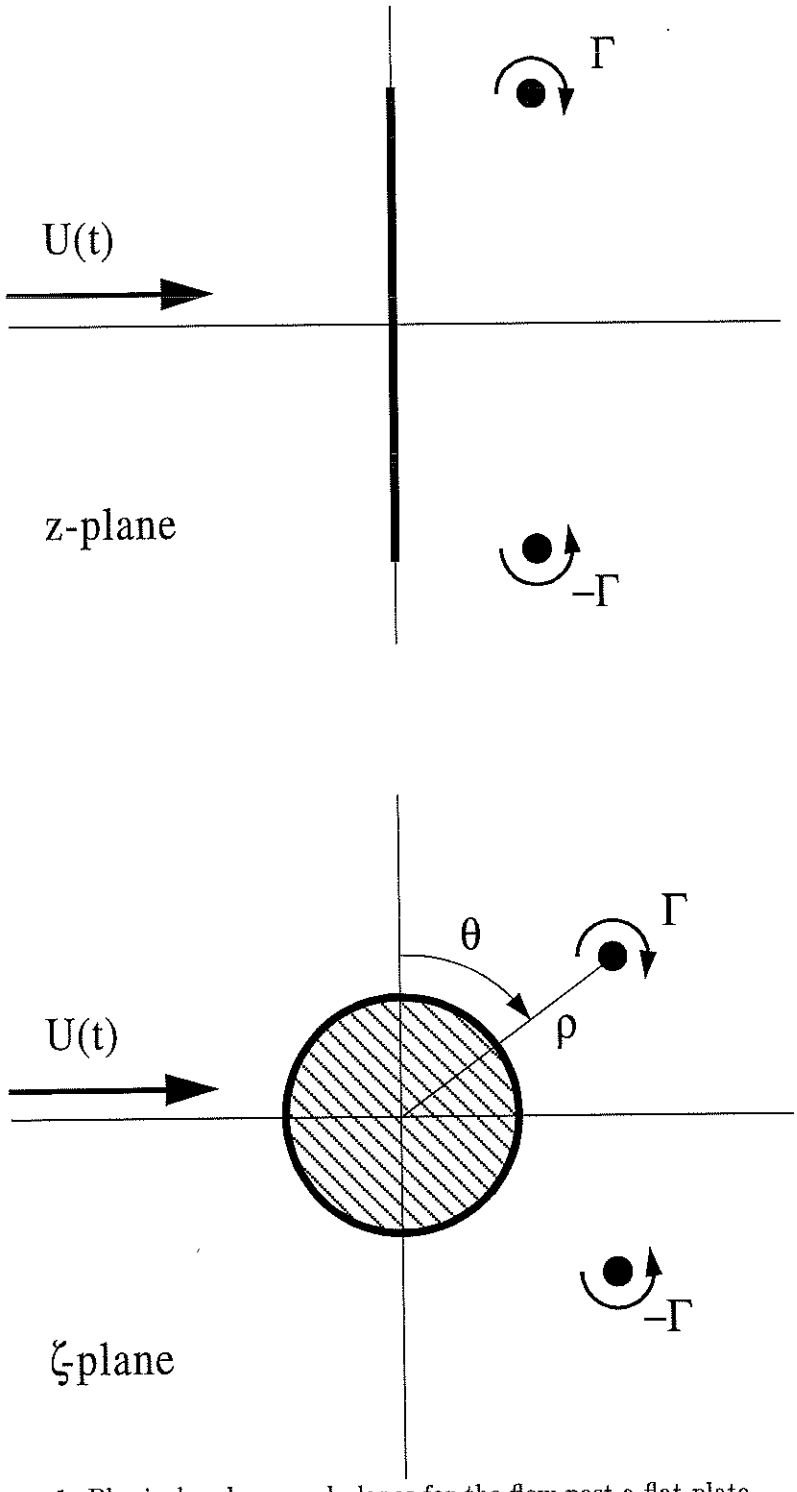


Figure 1: Physical and mapped planes for the flow past a flat plate.

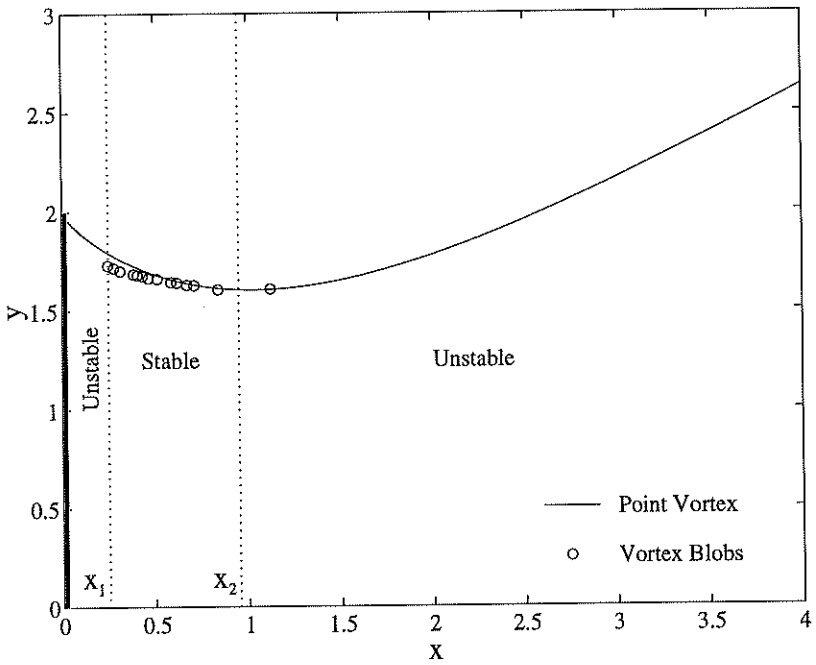


Figure 2: Locus of the fixed points.

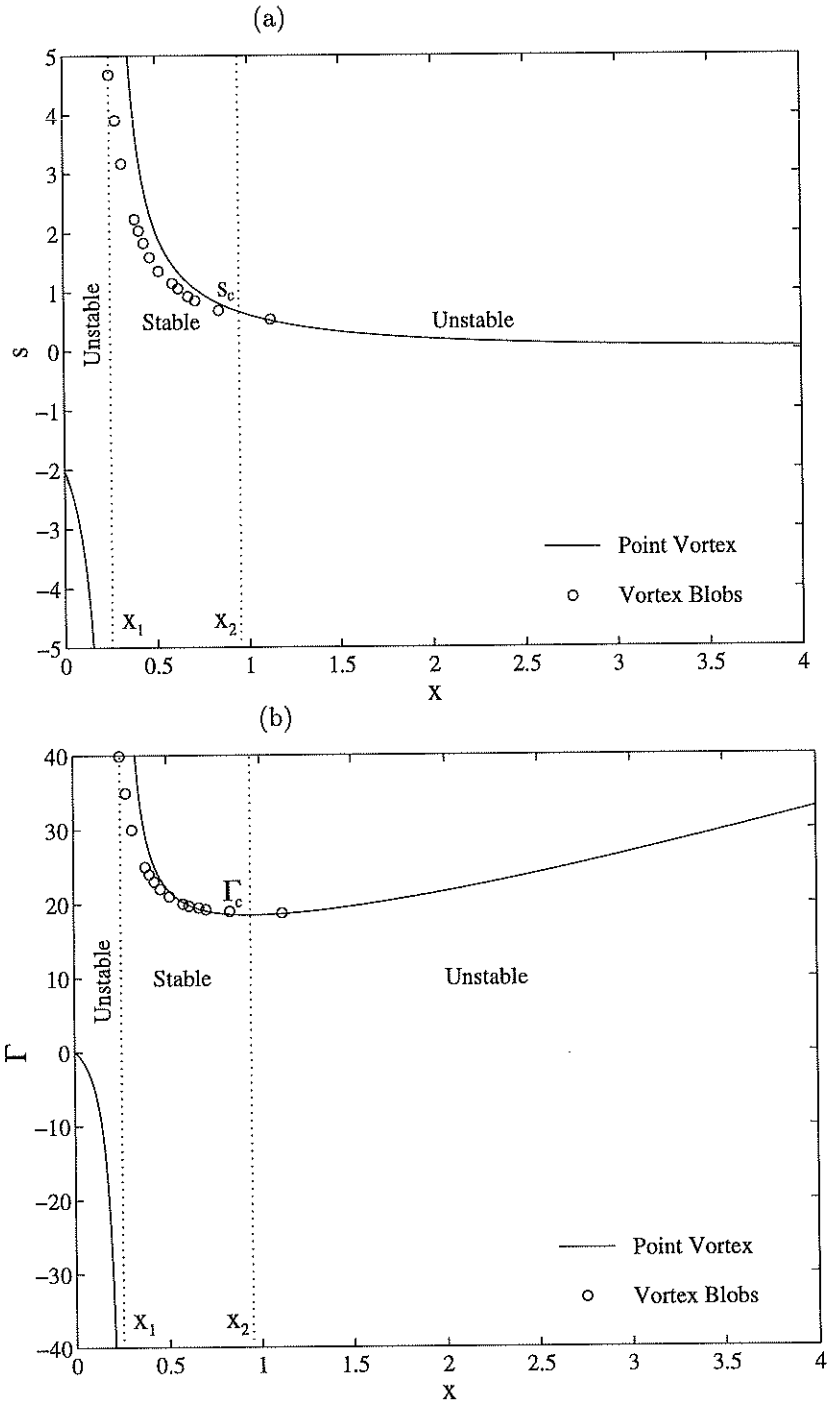


Figure 3: Flow quantities associated with the fixed points: Suction (a) and circulation (b).

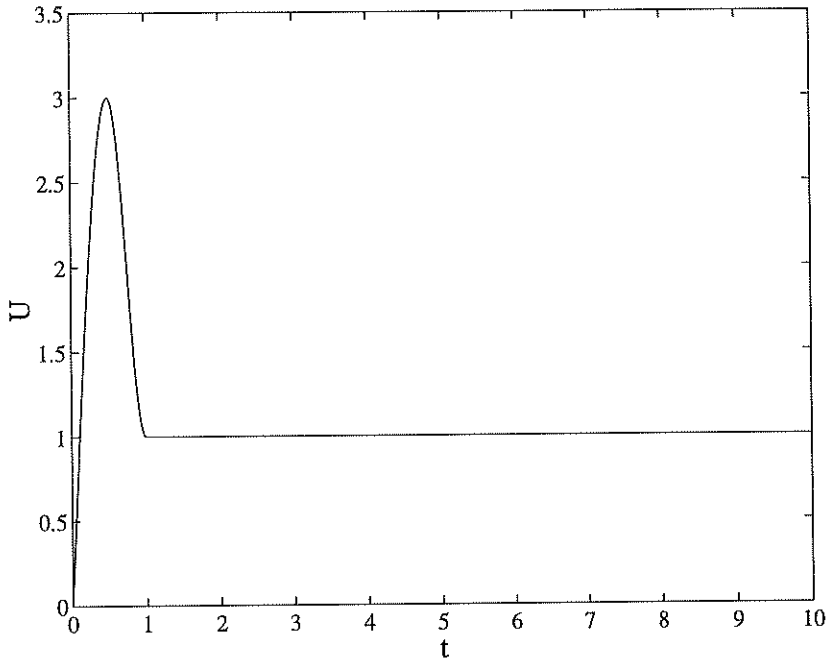


Figure 4: Free-stream velocity.

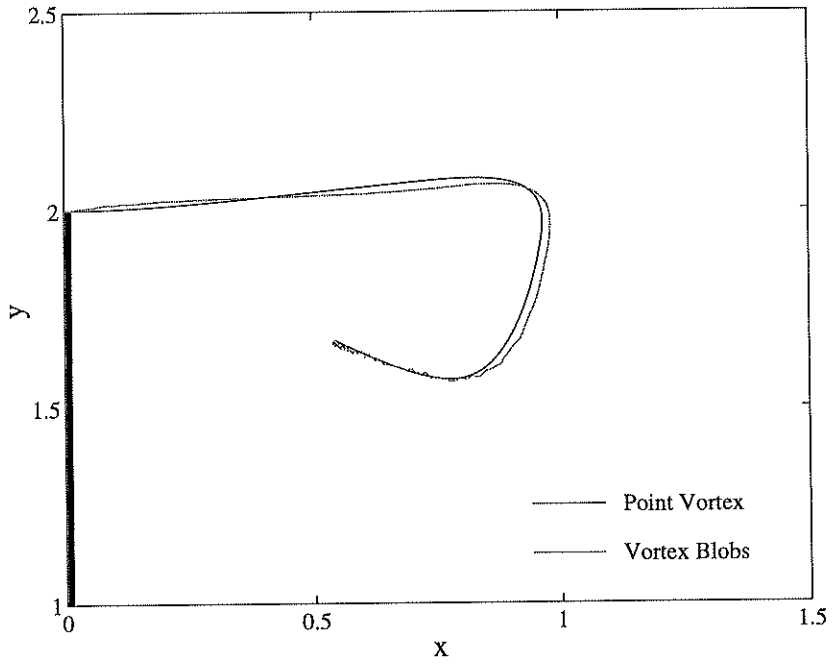


Figure 5: Comparison between the trajectory of the top vortex and the trajectory of the top center of circulation.

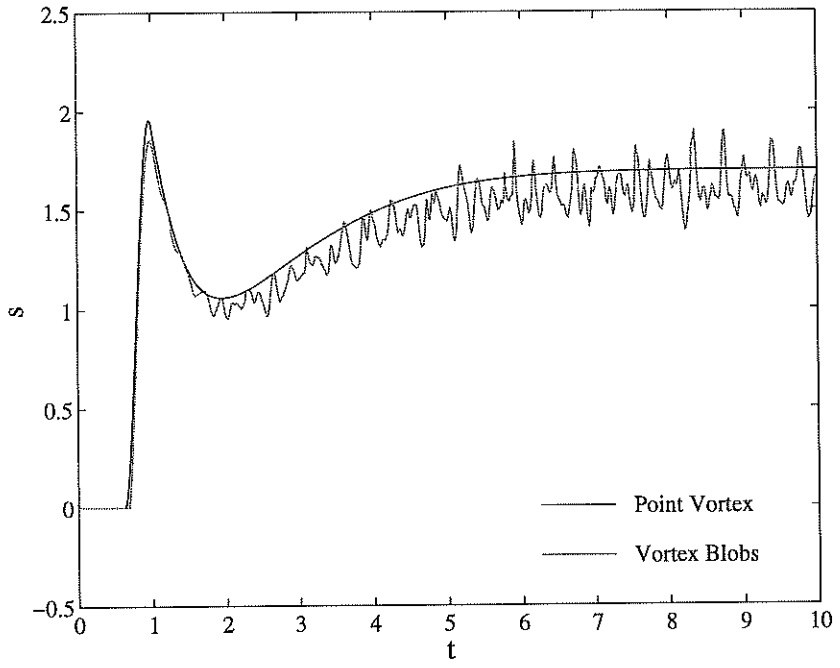


Figure 6: Comparison between the suction required to control the point vortex model and the suction required to control the vortex blob model.

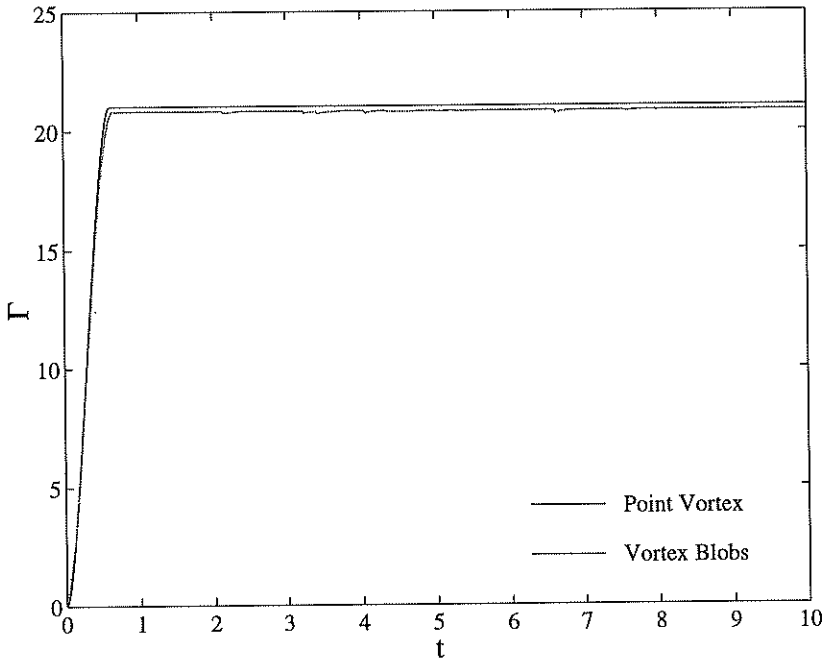


Figure 7: Comparison between the circulation of the top point vortex and the circulation of the top center of circulation.

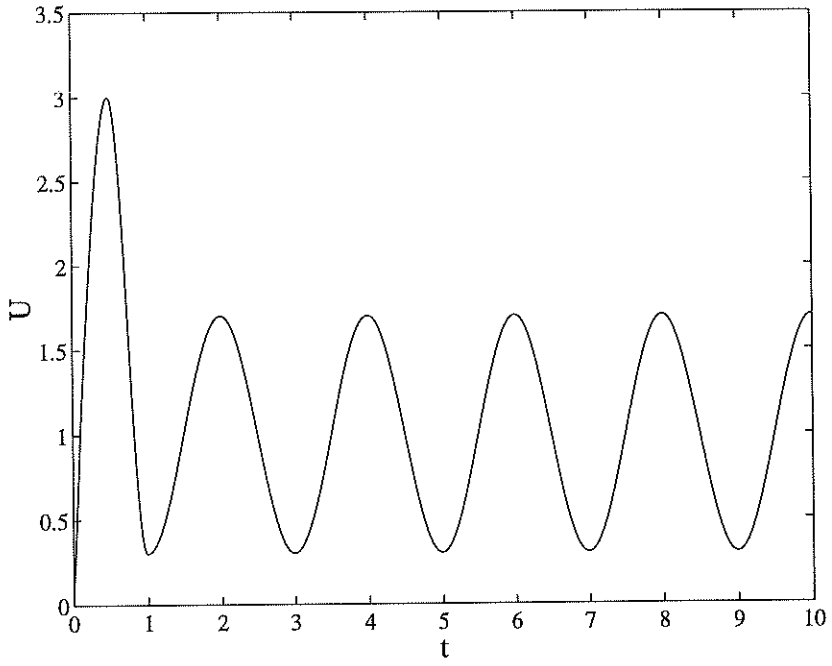


Figure 9: Free-stream velocity.

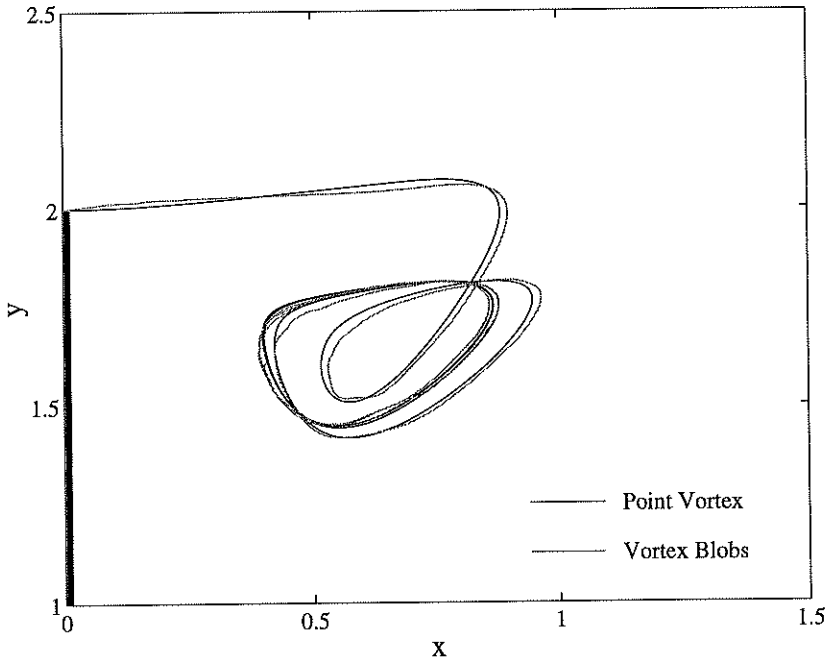


Figure 10: Comparison between the trajectory of the top vortex and the trajectory of the top center of circulation.

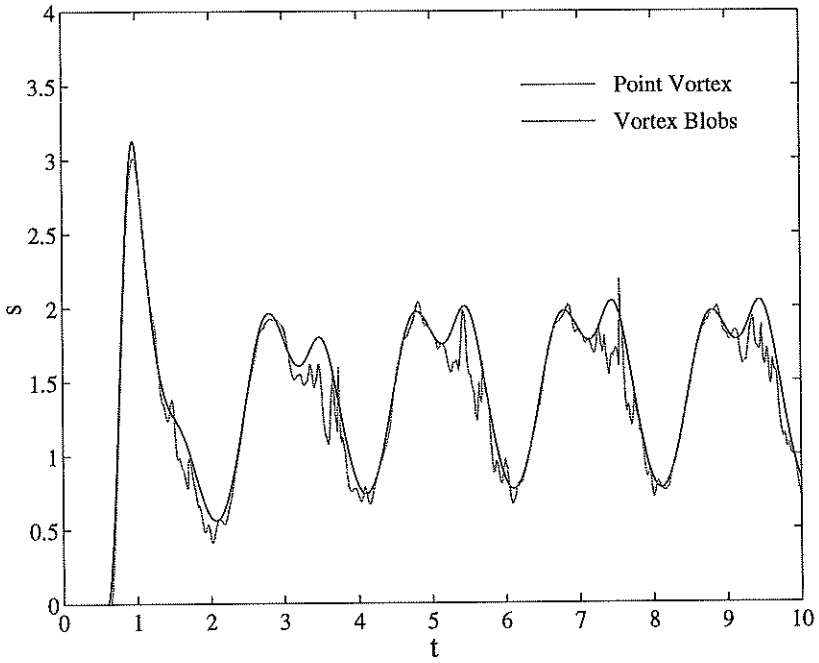


Figure 11: Comparison between the suction required to control the point vortex model and the suction required to control the vortex blob model.

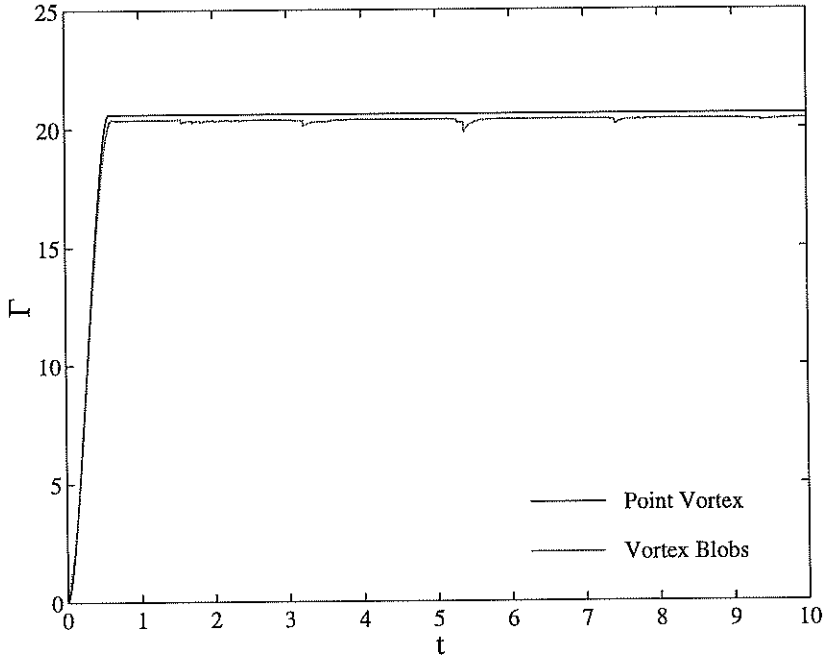


Figure 12: Comparison between the circulation of the top point vortex and the circulation of the top center of circulation.

## References


BROWN, C.E. & MICHAEL, W.H. 1954 Effect of leading-edge separation on the lift of a delta wing. *J. Aero. Sci.* **21**, 690–694.

BUSHNELL, D.M. 1992 Longitudinal vortex control — techniques and applications — The $32^{nd}$ Lanchester Lecture. *Aeronautical Journal* **96**, 293–312.

CAO, N-Z & AUBRY, N. 1993 Numerical simulation of a wake flow via a reduced system. FED-Vol. 149, Separated flows, ASME 1993

CHEIN, R. & CHUNG, J.N. 1988 Discrete-vortex simulation of flow over inclined and normal plates. *Computer & Fluids* **16**, 405–427.

CHORIN, A.J. 1973 Numerical study of slightly viscous flows. *J. Fluid Mech.* **57**, 785–796.

CLEMENTS, R.R. 1973 An inviscid model of two-dimensional vortex shedding. *J. Fluid Mech.* **57**, 321–336.

CORTELEZZI, L. 1995 On the active control of the wake past a plate with a suction point on the downstream wall. Submitted to: *J. Fluid Mech.*

CORTELEZZI, L., LEONARD, A. & DOYLE, J.C. 1994 An example of active circulation control of the unsteady separated flow past a semi-infinite plate. *J. Fluid Mech.* **260**, 127–154.

CORTELEZZI, L. & LEONARD, A. 1993 Point vortex model for the unsteady separated flow past a semi-infinite plate with transverse motion. *Fluid Dynamics Research* **11**, 263–295.

CORTELEZZI, L. 1993 A theoretical and numerical study on active wake control. Ph.D. Thesis, California Institute of Technology.

GAD-EL-HAK, M. & BUSHNELL, D.M. 1991 Separation control: review. *ASME J. Fluids Eng.* **113**, 5–30.

GOPALKRISHNAN, R., TRIANTAFYLLOU, M.S., TRIANTAFYLLOU, G.S. & BARRETT, D. 1994 Active vorticity control in a shear flow using a flapping foil. *J. Fluid Mech.* **274**, 1–21.

GUCKENHEIMER, J. & HOLMES, P. 1983 Nonlinear oscillations, dynamical systems, and bifurcation of vector fields. Springer-Verlag, New York

GUNZBURGER, M.D. 1995 Flow control. Springer-Verlag, New York

HALD, O.H. 1979 Convergence of vortex methods for Euler equations. II. *Siam J. Numer. Anal.* **16**, 726–755.

KIYA, M. & ARIE, M. 1977 A contribution to an inviscid vortex-shedding model for an inclined flat plate in uniform flow. *J. Fluid Mech.* **82**, 223.

KOOCHESFAHANI, M.M. & DIMOTAKIS, P.E. 1988 A cancelation experiment in a forced turbulent shear layer. *First National Fluid Dynamics Congress July 25-28, 1988, Cincinnati, Ohio.* AIAA Paper No. 88-3713-CP.

KRASNY, R. 1991 Vortex sheet computations: roll-up, wakes, separation. *Lect. Appl. Math.* **28**, 385–401.

LISOSKI, D.L. 1993 Nominally 2-dimensional flow about a normal flat plate. Ph.D. Thesis, California Institute of Technology.

ONGOREN, A. & ROCKWELL, D. 1988a Flow structure from an oscillating cylinder Part 1. Mechanisms of phase shift and recovery in the near wake. *J. Fluid Mech.* **191**, 197–223.

ONGOREN, A. & ROCKWELL, D. 1988b Flow structure from an oscillating cylinder Part 2. Mode competition in the near wake. *J. Fluid Mech.* **191**, 225–245.

RAJAEE, M., KARLSSON, S.K.F. & SIROVICH, L. 1994 Low-dimensional description of free-shear-flow coherent structures and their dynamical behavior. *J. Fluid Mech.* **258**, 1–29.

RAO, D.M. 1987 Vortical flow management techniques. *Prog. Aerospace Sci.* **24**, 173–224.

ROSSOW, V.J. 1977 Lift enhancement by an external trapped vortex. *10th Fluid and Plasmadynamics Conference, June 27-29, 1977, Albuquerque, New Mexico.* AIAA Paper No. 77-672.

ROUSSOPOULOS, K. 1993 Feedback control of vortex shedding at low Reynolds numbers. *J. Fluid Mech.* **248**, 267–296.

ROTT, N. 1956 Diffraction of a weak shock with vortex generation. *J. Fluid Mech.* **1**, 111–128.

SARPKAYA, T. 1975 An inviscid model of two-dimensional vortex shedding for transient and asymptotically steady separated flow over an inclined plate. *J. Fluid Mech.* **68**, 109.

SARPKAYA, T. 1989 Computational methods with vortices – The 1988 Freeman Scholar Lecture. *ASME J. Fluids Eng.* **111**, 5–52.

SLOMSKI, J.F. & COLEMAN, R.M. 1993 Numerical simulation of vortex generation and capture above an airfoil. *31st Aerospace Sciences Meeting and Exhibit, January 11-14, 1993, Reno, Nevada.* AIAA Paper No. 93-864.

TOKUMARU, P.T. & DIMOTAKIS, P.E. 1991 Rotary oscillation control of a cylinder wake. *J. Fluid Mech.* **224**, 77–90.